scientific reports

Check for updates

OPEN

Comparative analysis of organoid, air-liquid interface, and direct infection models for studying pathogen–host interactions in endometrial tissue

Xin Zhang, Linyuan Fan✉, Li Zhang & Zhaohui Liu✉

The endometrium is a critical component of female reproductive health. Endometritis can significantly affect women's health, leading to complications such as infertility, pregnancy failure, and intrauterine adhesions. Therefore, establishing a reliable and effective model of endometritis is essential for advancing research in female reproductive health. The air-liquid interface culture models epithelial exposure to both air and medium, supporting the study of apical-basal polarity and immune responses, but lacks the three-dimensional structure of organoids. Microinjection delivers bacteria directly into the organoid lumen, facilitating the study of bacterial invasion and replication, though it requires advanced technical skills and may not fully replicate natural infections. The direct infection of organoids in suspension culture offers a more realistic model of ascending infections by exposing the basal epithelial surfaces to bacteria, more closely mimicking in vivo conditions. Among the models tested, the direct infection method most accurately mirrors the progression of *E. coli* infection, showing its advantage in studying bacterial adhesion, replication, and epithelial barrier disruption. Our comparative analysis of microinjection, direct infection, and the ALI model highlighted distinct advantages and challenges associated with each. Microinjection offers precise delivery but is hindered by technical complexity and equipment demands. The ALI model, despite its efficacy, requires extended culture times and limits direct visualization of cell development. Conversely, the direct infection model, which involves the simple removal of Matrigel, proves to be user-friendly, cost-effective, and permits continuous observation of cell behavior. Nonetheless, the direct infection model still presents certain limitations that warrant further optimization.

Keywords Infection model, Endometrial organoids, Air-liquid interface, Transwell

Background

The endometrial epithelium plays a pivotal role in maintaining uterine homeostasis, supporting blastocyst implantation, and providing a barrier against ascending infections. Gaining a deep insight into its biological roles is vital for improving reproductive health outcomes. When the epithelium becomes dysfunctional, it may lead to several uterine conditions, such as infertility, repeated failures in implantation, the formation of intrauterine adhesions, or complications during pregnancy[1,2]. However, the challenges posed by the limitations of in vitro models and the ethical concerns associated with conducting in vivo experiments, particularly during gestation, significantly hinder human-based research efforts. These limitations prevent a full understanding of the molecular and cellular mechanisms that are essential for regulating endometrial epithelial function and physiology.

Organoids have recently emerged as essential models for studying epithelial biology, disease mechanisms, and embryo-maternal interactions. Endometrial epithelial cells are typically extracted using enzymatic

Department of Gynecology, Beijing Obstetrics and Gynecology Hospital, Capital Medical University, Beijing Maternal and Child Health Care Hospital, No. 251, Yaojiayuan Road, Chaoyang District, Beijing 100026, China. ✉email: fanlinyuan@ccmu.edu.cn; liuzhaohui@ccmu.edu.cn

digestion and mechanical processes, then embedded in Matrigel to create three-dimensional endometrial organoids (EOs)[3]. When cultured in growth-factor-enriched media, these organoids undergo self-organization, proliferation, and differentiation into more complex structures. Importantly, EOs preserve critical attributes of the native endometrial epithelium, such as tissue structure, cell composition, gene expression patterns, hormone sensitivity, and protein secretion profiles during growth[4]. As a result, organoids are seen as more reflective of clinical outcomes and phenotypes than traditional two-dimensional cultures, making them invaluable for biomarker identification and functional testing. A hallmark of Matrigel-embedded organoids is their hollow, cyst-like structure. Research has shown that EOs exhibit apical-basal polarity, with the basal side attached to the Matrigel and the apical surface forming an internal lumen. However, this polarity complicates the study of epithelial-embryo interactions and infections by pathogens within the uterine cavity[5].

To overcome the challenges of studying infections in organoids, a microinjection technique was introduced. This method allows the introduction or removal of factors from the organoid's basal surface or lumen, as well as the delivery of pathogens for infection research[6,7]. For example, the microinjection of *H pylori* into organoids has enabled the examination of its invasion and replication within epithelial cells, shedding light on the pathogen's mechanisms[8]. Despite its usefulness, the technique poses technical challenges, such as requiring organoids to reach a larger size and the risk of contamination in the basal compartment. Additionally, ensuring uniform exposure of injected agents within the organoid lumen is hindered by the variability in organoid sizes. To overcome these limitations, a suspension culture method was devised to reverse the polarity of EOs. This technique involves removing the Matrigel and culturing the organoids in low-attachment plates, which reverses the polarity of EOs without compromising their hormonal responsiveness or viability. These polarity-reversed EOs retain histological and physiological characteristics similar to those of the uterine epithelium in vivo, including secretory cell differentiation in response to hormonal cues[9]. This approach has been applied successfully to both human and mouse EOs, with polarity inversion occurring after Matrigel removal and one week in suspension culture[5].

The ALI culture technique has been employed to establish epithelial polarity by seeding primary epithelial cells onto Transwell inserts, where they grow until they reach confluence. At this stage, the medium is removed from the apical side, while nutrients are supplied to the cells through the basal surface via the porous Transwell membrane, forming the ALI culture[10]. Epithelial cells cultured under these conditions exhibit near-natural differentiation, as demonstrated in upper airway studies. For example, in human bronchial epithelial cells (HBECs), the ALI culture fosters the development of apical-basal polarity[11,12] leading to the differentiation of cells into secretory goblet cells and ciliated epithelial cells[13,14]. Moreover, this method supports the organization of cells into a pseudostratified columnar epithelium.

Ascending *E. coli* infections from the vaginal canal to the uterus represent a major health concern in both pregnant and non-pregnant individuals[15]. In non-pregnant individuals, such infections can result in pelvic inflammatory disease, intrauterine adhesions, and recurrent implantation failure[16]. During pregnancy, they are associated with serious complications such as maternal and neonatal sepsis, miscarriage, and preterm birth. To investigate the effects of different infection methods, three culture techniques were used to assess the interaction between endometrial tissue and Escherichia coli. These approaches represent distinct models of endometrial epithelial pathology. Organoids offer a valuable platform for studying uterine cavity interactions due to their ability to form functional interfaces with external stimuli.

Methods

Establishment of endometrial organoids

This study was conducted in accordance with the Declaration of Helsinki. All analyses involving patient and human samples adhered to the guidelines and procedures of the Beijing Obstetrics and Gynecology Hospital, Capital Medical University. The Institutional Review Board (IRB number:2023-KY-011-02), approved the appropriate licenses and protocols, and informed consent was obtained from all participating patients. Endometrial samples were collected from premenopausal women ($n=3$) undergoing routine hysterectomy for benign uterine conditions. These women had not taken any hormonal drugs in the three months prior to tissue collection. The endometrial samples were histologically classified as normal proliferative by pathologists at Beijing Obstetrics and Gynecology Hospital. Fresh endometrial tissue was collected during surgeries and processed immediately to ensure the preservation of cellular characteristics. The tissue was enzymatically digested at 37 °C for 45 min using collagenase II (1 mg/mL, Sigma, C2-28-100MG) and collagenase IV (1 mg/mL, Sigma, C4-28-100MG), in combination with a ROCK inhibitor (10μM, Y27632, MCE, HY-10071/CS-0131) to facilitate single-cell dissociation and prevent cell aggregation. The collagenase concentration and digestion time were optimized to ensure effective tissue dissociation while maintaining cell viability. After enzymatic digestion, the digested tissue was filtered through a 100 μm cell strainer to remove undigested tissue fragments, and the resulting single-cell suspension was collected. The entire dissociation process was carried out in a sterile environment, and cell viability was regularly checked using trypan blue exclusion assay to ensure the high quality of the dissociated cells. To ensure proper cell encapsulation for organoid culture, the cell suspension was resuspended in Matrigel (70%, Corning, 356255, no phenol red) and plated in a 24-well plate. The use of Matrigel provides a suitable three-dimensional environment for organoid formation, mimicking the in vivo tissue architecture. Three drops of this Matrigel-cell suspension were plated into each well of a 24-well plate, which was overlaid with 500μL of media containing DMEM/F12 (HyClone, SH30272.01), B27 (1X, Gibco, 17504-044), N2 supplement (1X, Gibco, 17502-048), 500nM A83-01 (MCE, HY-10432), 250 μg/mL EGF (MCE, HY-P7109), 250 μg/mL Rspondin-1 (MCE, HY-P7114), and 100 μg/mL Noggin (MCE, HY-P7051A). Organoids formed within 3–4 days and were passaged according to their growth and confluence, which were monitored using both an optical microscope and a fluorescence microscope (OLYMPUS).

Generation and propagation of Apical-Out endometrial organoids (AO-EOs)

To generate apical-out endometrial organoids (AO-EOs), the growth medium was first aspirated, and cell recovery solution was added to the culture. The organoid-cell mixture was then transferred into Eppendorf tubes using wide-bore 1 mL pipette tips. The tubes were gently rotated at 4 °C for 1 h to allow complete dissociation. Following this, the organoids were pelleted by centrifugation at 100 g for 5 min and washed with DMEM/F12 to remove the recovery solution. The washed organoids were resuspended in a medium supplemented with the ROCK inhibitor Y27632, which supports cell survival and prevents anoik is in suspension cultures. These organoids were then seeded into ultra-low attachment plates (Corning, Cat. No. 3473) to establish a suspension culture. To avoid organoid clumping, gentle agitation using a pipette was performed twice daily. The growth medium was replaced every other day to maintain optimal conditions for organoid proliferation and apical-out orientation.

Establishment of ALI culture system

Organoids were first removed from Matrigel and dissociated into single cells using TrypLE (Gibco, 12604021). To ensure cell viability, the cell suspension was diluted in trypan blue, and the live cells were counted using a hemocytometer. A total of 5×10^5 viable cells were seeded onto the porous membranes of 12-well Transwell inserts (0.4 μm pore size, Thermo Fisher, 141002), with 250μL of culture medium added to the apical side of the insert and 500μL to the basolateral chamber. After 72 h of culture, the medium in the apical compartment was carefully aspirated to establish the ALI culture, leaving only 500μL of medium in the basolateral chamber. The basolateral medium was replaced every three days to maintain optimal cell growth and differentiation.

Hormone treatment of organoids

To examine the hormone responsiveness of EOs following passaging, 10,000 cells per Matrigel droplet were plated in 24-well plates (3 droplets per well) and allowed to establish into organoids over 3 d in organoid medium. We chose 10nM E2 (estradiol) and the corresponding concentration of P4 (progesterone) based on previous studies that demonstrated these levels effectively simulate the hormonal environment necessary for the physiological functions of endometrial cells in vitro[17]. EOs were then treated with either 10nM estradiol (MCE, HY-B0141) or control for 3 d. Following this, organoids were treated with either 10nM E2 and 1μM P4 (Progesterone, MCE, HY-N0437) (E2 + P4), 10nM E2, for a further 4 d. Each treatment was performed in triplicate wells with a fourth well for each treatment used for histology purposes.

Co-culture of organoids with bacteria

Escherichia coli (ATCC-25922) was obtained from the Microecology Laboratory of Beijing Obstetrics and Gynecology Hospital and routinely cultured on LB agar plates at 37 °C. For bacterial growth, isolated colonies were picked from agar plates and inoculated into LB broth (Solarbio, L8291), followed by incubation at 37 °C with shaking. EOs were removed from Matrigel by treating them with cell recovery solution and then washed thoroughly with DMEM/F12 medium. The *E. coli* concentration was measured using a spectrophotometer (OD600). The bacteria were used in their exponential phase to ensure maximum viability and infectivity. We used an MOI of 1 for the infection experiments. The EOs were subsequently resuspended in organoid culture medium. To initiate the co-culture, EOs were combined with bacterial cells in a tissue culture incubator and rotated for 1 h to promote bacterial interaction. After the incubation, excess bacterial cells were removed by washing the organoids with PBS multiple times to minimize non-adherent bacteria. The co-cultured organoids were then incubated for a recovery period of 24 h, with fresh medium added every other day. At predetermined timepoints, 500μL of the culture medium supernatant was collected for ELISA to quantify cytokine or protein levels related to bacterial infection.

Total RNA isolation and real-time quantitative PCR

Total RNA was extracted using the Trizol reagent (RNA Extraction Kit, AG11701, Accurate Biology Co., Ltd.) according to the manufacturer's protocol. The isolated RNA was then reverse transcribed into complementary DNA (cDNA) using the Reverse Transcription Kit (AG11728, Accurate Biology Co., Ltd.). Real-time quantitative PCR (qPCR) was conducted using SYBR Green dye (AG11701, Accurate Biology Co., Ltd.) on an ABI7500 system. The gene expression levels were calculated using the comparative threshold cycle (Ct) method. Primers for the genes of interest are listed in Table 1. Each reaction was performed in triplicate to ensure reproducibility and minimize variation.

RNA-seq analysis

Total RNA was extracted from EOs using Trizol reagent according to standard protocols. RNA integrity was assessed with the RNA Nano 6000 Assay Kit on the Bioanalyzer 2100 system (Agilent Technologies, CA, USA), ensuring high-quality RNA for downstream applications. The quality control parameters included an A260/A280 ratio ≥ 1.8, A260/A230 ratio ≥ 2.0, and an RNA Integrity Number (RIN) ≥ 8.0. For RNA sequencing, 1 μg of RNA was used for library preparation. mRNA was enriched using oligo(dT) beads, fragmented, and reverse transcribed to generate cDNA. The cDNA was then subjected to end repair, adapter ligation, and amplification to construct the sequencing library. The library's quality was assessed using the Agilent Bioanalyzer and Qubit Fluorometer, and only libraries with a size range of 300–500 bp were selected for sequencing. RNA sequencing was performed on the Illumina HiSeq 2500 platform (Illumina, Inc., San Diego, CA, USA) with paired-end sequencing (2 × 150 bp). Raw data were processed with FastQC for quality control, and reads were aligned to the reference genome using STAR. Differential expression analysis was conducted using DESeq2, with differentially expressed genes (DEGs) identified based on a fold change > 2 and a false discovery rate (FDR) < 0.05. KEGG

Primer	Accession number	Product size	Sequence (5′-3′)
Human_ ESR	XM_054354491	147	F: TGCCCTACTACCTGGAGAAC
			R: CCATAGCCATACTTCCCTTGTC
Human_ PGR	XM_054369129	106	F: GAAGGGCAGCACAACTACTTA
			R: CAGCCTGACAGCACTTTCTA
Human_ LIF	NM_002309	233	F: TCTTGGCGGCAGGAGTTG
			R: CTTGTCCAGGTTGTTGGGGA
Human_ PAEP	NM_001018049	296	F: GCGACCAACAACATCTCCCT
			R: GCCAGGTACTGGCACATCAT
Human_HSPA1B	NM_005346	131	F: GCGAGGCGGACAAGAAGAA
			R: GATGGGGTTACACACCTGCT
Human_DUSP5	NM_004419	132	F: GCCAGCTTATGACCAGGGTG
			R: GTCCGTCGGGAGACATTCAG
Human_ ATF4	NM_182810	153	F: ATGACCGAAATGAGCTTCCTG
			R: GCTGGAGAACCCATGAGGT
Human_ JUNB	NM_002229	128	F: ACAAACTCCTGAAACCGAGCC
			R: CGAGCCCTGACCAGAAAAGTA
Human_ MAPK	NM_001286124	168	F: CGAGCCAGGCAGTGATTTGA
			R: CAGTAACGAGGGAGGGCTTC
Human_IL8	NM_000584	248	F: TCTGCAGCTCTGTGTGAAGG
			R: TTCTCAGCCCTCTTCAAAAACT
Human_ TNF-α	NM_000594	185	F: CACAGTGAAGTGCTGGCAAC
			R: AGGAAGGCCTAAGGTCCACT
Human_ GAPDH	NM_001357943	110	F: GACACCCACTCCTCCACCTTT
			R: ACCACCCTGTTGCTGTAGCC

Table 1. Primers used for qPCR. Gene annotation: ESR, Estrogen receptor; PGR, Progesterone receptor; PAEP, Progestagen associated endometrial protein; HSPA1B, Heat shock protein family A (Hsp70) member 1B; DUSP5, Dual specificity phosphatase 5; IL8, Interleukin-8; TNF-α, Tumor necrosis factor; GAPDH, Glyceraldehyde-3-phosphate dehydrogenase.

pathway analysis was performed using the clusterProfiler R package with an FDR threshold of 0.05 to assess the statistical significance of enriched pathways. The primers used for qPCR are listed in Table 1.

ELISA assay

The ELISA assay utilized antibodies specific to human TNF-α (NeoBioscience, ECC102a), IL-8 (NeoBioscience, EHC008.96), and IFN-γ (NeoBioscience, EHC102g.96), which were immobilized in 96-well plates according to the manufacturer's instructions. Organoid-conditioned medium and protein standards were added to the wells, allowing the target proteins to bind to the immobilized antibodies for 2.5 h at room temperature. Following this incubation, biotinylated secondary antibodies were added and allowed to incubate for an additional hour. After incubation, the wells were washed four times with 1× wash solution to remove unbound material. The absorbance at 450 nm was measured using a microplate reader. All experiments were performed in triplicate to ensure statistical reliability.

Statistical analysis

Significant differences among the three experimental groups were determined using one-way analysis of variance (ANOVA) for comparisons involving three sets of data and t-tests for comparisons involving two sets of data. All statistical analyses were performed using GraphPad Prism 9, and the data are presented as mean ± standard error of the mean (SEM). Differences were considered statistically significant at $P < 0.05$.

Results

Establishment of human endometrial organoids

Endometrial epithelial cells were isolated from the uterine tissues of premenopausal women undergoing treatment for benign uterine lesions. The endometrial samples comprised a mixture of proliferative and secretory tissues. The epithelial cells were mixed with Matrigel at a volume ratio of 3:7 and seeded into 24-well plates, followed by culturing in organoid growth medium (Fig. 1). After approximately 8 days of culture, the organoids were digested into cell clusters, mixed with Matrigel, and reseeded into 24-well plates for further cultivation. Daily observations and photographs were recorded. Organoids began to form the day after seeding, with a significant increase in proliferation observed by day 5, continuing until day 7 (Fig. 1a). Organoids were cultured further and passaged up to passage 20, with no significant changes in formation rate, morphology, or size following thawing from cryopreservation (Fig. 1b). Statistical analysis indicated that after 7 days of culture, approximately 93.0% of organoids exhibited a diameter greater than 100 μm, with the majority ranging from 100

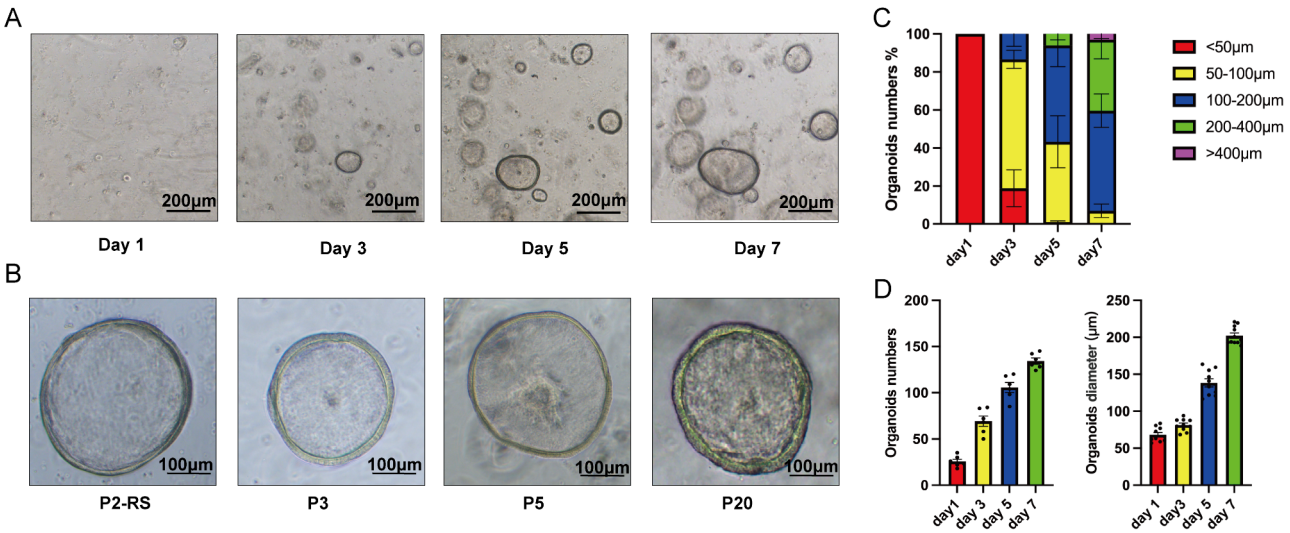

Fig. 1. Establishment and long-term stable passage of human endometrial organoids. (**A**) Brightfield images of organoids formed within 7 days. Scale bar: 100 μm. (**B**) Brightfield images of organoids at different passages, demonstrating long-term expansion. Scale bar: 200 μm. Organoids from passage 3(P3), after thawing of P2, passage 5 (P5), and passage 20 (P20) are shown. The morphology and structure of the organoids changed after passage and revival. (**C**) The proportion of organoids with different diameters formed on different days. (**E**) Diameter of organoids on days 1, 3, 5, and 7, and the number of organoids per drop of Matrigel on days 1, 3, 5, and 7. The results are shown as the mean ± SEM of triplicate samples and are representative of three independent experiments. Statistical significance is indicated as follows: $^{*}P \leq 0.05$, $^{**}P \leq 0.01$, $^{***}P \leq 0.001$.

to 200 μm, accounting for approximately 52.6% (Fig. 1c). The average diameter was 200 μm, with approximately 135 organoids per droplet (Fig. 1d).

Organoid hormonal responsiveness

According to previous reports, EOs form spherical structures, with the basolateral epithelial surface facing outward in contact with Matrigel, while the apical surface faces inward toward the organoid lumen[5]. To maintain the integrity of EOs during removal from Matrigel, a cell recovery solution was employed to dissociate the Matrigel and release the organoids without disrupting their three-dimensional structure. The EOs were subsequently transferred to suspension culture in growth medium using ultra-low attachment plates. Visible morphological changes were noted in EOs during suspension culture. While Matrigel-embedded organoids maintained a single-layered epithelium with a central lumen, the central lumen of suspension-cultured EOs disappeared, resulting in solid structures. Scanning electron microscopy (SEM) further confirmed the polarity reversal in suspension-cultured organoids, with the outward-facing apical surface covered with microvilli, whereas the outward surface of ALI organoids appeared smooth. To construct the ALI model, organoids were similarly released from Matrigel, dissociated into cell clusters, and cultured in transwell chambers. During the culture process, partially dissociated organoids fragmented, and the cells spread across the transwell membrane. SEM revealed that cells in the ALI culture expanded, with their surface also covered with microvilli (Fig. 2a).

Estradiol (E2) regulates both estrogen receptor (ER) and progesterone receptor (PR), which are encoded by the ESR and PGR genes, respectively. At the end of a 14-day normal hormonal treatment mimicking the follicular phase of the menstrual cycle, we assessed the expression of the estrogen receptor (ER, Fig. 2B) and progesterone receptor (PR, Fig. 2B) using qPCR across three different culture models. Compared to the control group, ESR mRNA expression increased approximately 5-fold in the AI model and 7-fold in the AO model after E2 treatment, while the ALI model showed an approximately 2.6-fold increase ($p < 0.05$). Similarly, following E2 + P4 treatment, PGR mRNA expression increased approximately 5-fold in the AI model, 15-fold in the AO model, and about 7-fold in the ALI model compared to the control group ($p < 0.05$) (Fig. 2B). Additionally, ESR expression in the E2 treatment group (proliferative phase) was higher than that in the E2 + P4 treatment group (secretory phase). Fluorescent qPCR was further employed to measure the expression levels of genes associated with secretory-phase markers in the epithelium. The expression levels of progesterone-associated proteins PAEP and LIF increased in the AO, AI, and ALI secretory-phase models compared to the control group ($p < 0.05$), indicating that all three models responded to hormonal treatment, promoting cell proliferation and secretory-phase changes (Fig. 2C).

Comparison of three infection models

Different methods were employed for direct infection, including microinjection, direct infection following polarity inversion, and ALI infection. In the microinjection method, *E. coli* was directly injected into the

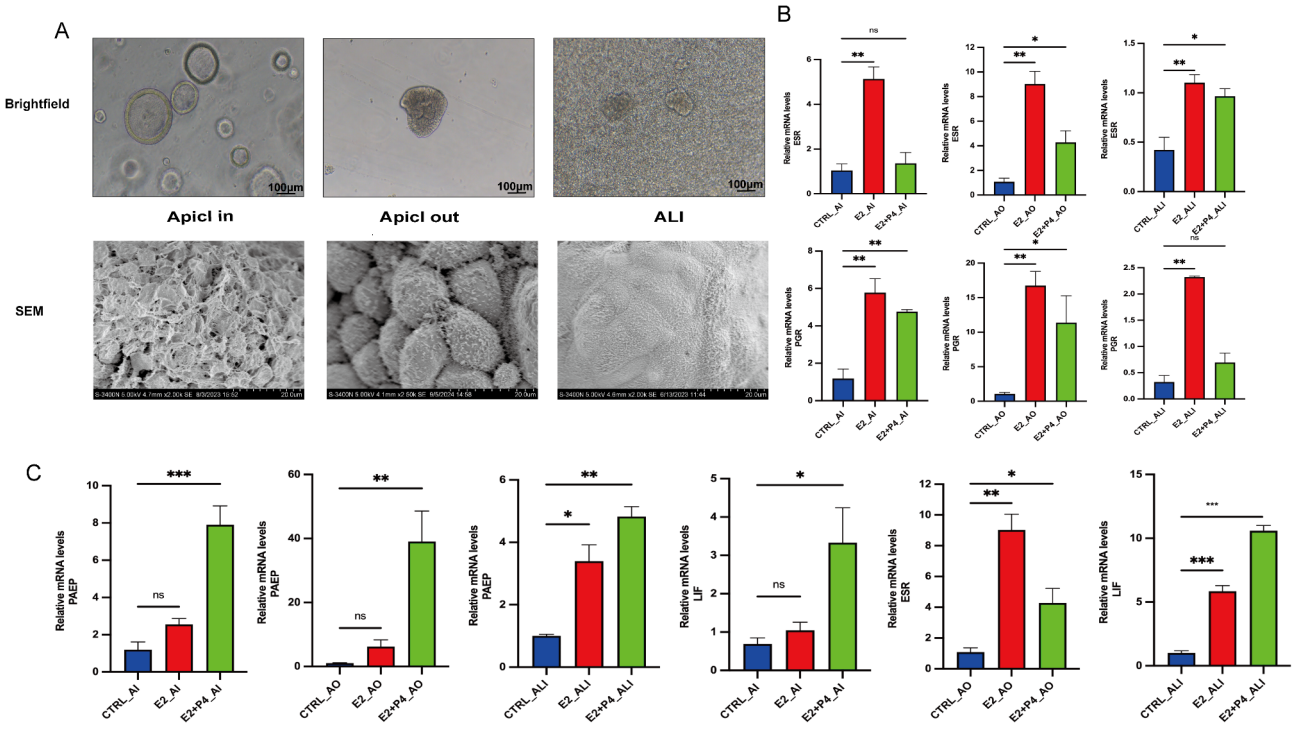

Fig. 2. Human endometrial organoids recapitulate the in vivo phenotype of endometrial glands. (**A**) Brightfield images of organoids in *Apical-in*, *Apical-out*, and ALI (air-liquid interface) conditions. Scale bar: 100 µm. Scanning Electron Microscope (SEM) images show that the *Apical-out* model displays abundant microvilli, while the ALI model exhibits fewer microvilli compared to the *Apical-out*. In contrast, cells in the *Apical-in* model display tight junctions. (**B**–**C**) Organoids were observed after treatment with sex hormones to mimic the follicular phase of a normal menstrual cycle. RT-PCR analysis of RNA isolated from organoid cultures treated as described in the methods. Human endometrial epithelial organoids were responsive to ovarian steroid hormones, with relative mRNA expression of ESR, PGR, PAEP, and LIF in hormone-treated organoids. The results represent one of three independent experiments. Data are presented as means ± SEM. Data are means ± SEMs. $^{*}P \leq 0.05$, $^{**}P \leq 0.01$, $^{***}P \leq 0.001$.

organoids using a needle. It was observed that the *E. coli* remained confined within the organoids, with all injected organoids displaying a trace of the injection (Fig. 3A). For the direct infection method, the Matrigel was removed, and pathogens were used to infect the organoids, where bacteria were seen adhering around the organoids (Fig. 3B). The ALI infection involved breaking up the organoids and spreading them on transwell plates for pathogen infection (Fig. 3C). After infection, the supernatant was collected to measure inflammatory cytokines. Compared to the control group, TNF-α levels increased in all three infection methods, with the smallest increase observed in the apical-in(AI) model and the highest in the ALI model. For IL-8, the lowest increase was noted in the ALI model, while the apical-out (AO) model showed the highest increase. Following infection, qPCR was used to measure changes in TNF-α and IL-8 levels across the three different infection methods. However, in the AI model, *E. coli* remained confined within the organoid lumen, and rapid bacterial growth led to early organoid death. In the ALI model, due to the small number of cells, the cells died quickly. The inflammatory response was most intense in the AO model (Fig. 3D).

Signaling pathway alterations after infection

Applying a threshold of 1.5-fold change and a false discovery rate of < 0.05, the analysis identified 122 upregulated genes and 8 downregulated genes in the *E. coli*-treated group compared to the control group (Fig. 4A). The top 20 significantly upregulated KEGG pathways were selected from the enrichment results of the infected group, and a bar chart was created. Analysis revealed predominant enrichment of the MAPK signaling pathway post-infection in the KEGG pathway analysis. (Fig. 4B, C). Upregulated genes among the differentially expressed genes were selected to create a heat map and validated using qPCR. Post-infection, members of the heat shock protein 70 (HSP70) family, particularly HSPA1B, and the transcription factor ATF4 exhibited increased expression ($p < 0.05$). Furthermore, the expression of DUSP5, a gene associated with DNA damage repair, was also elevated ($p < 0.05$) (Fig. 4D). For the heat shock protein HSPA1B, the response was strongest in the AO model, followed by ALI, with the weakest response observed in the AI model. This trend was similarly noted for the transcription factors ATF4 and DUSP5 ($p < 0.05$) (Fig. 4E).

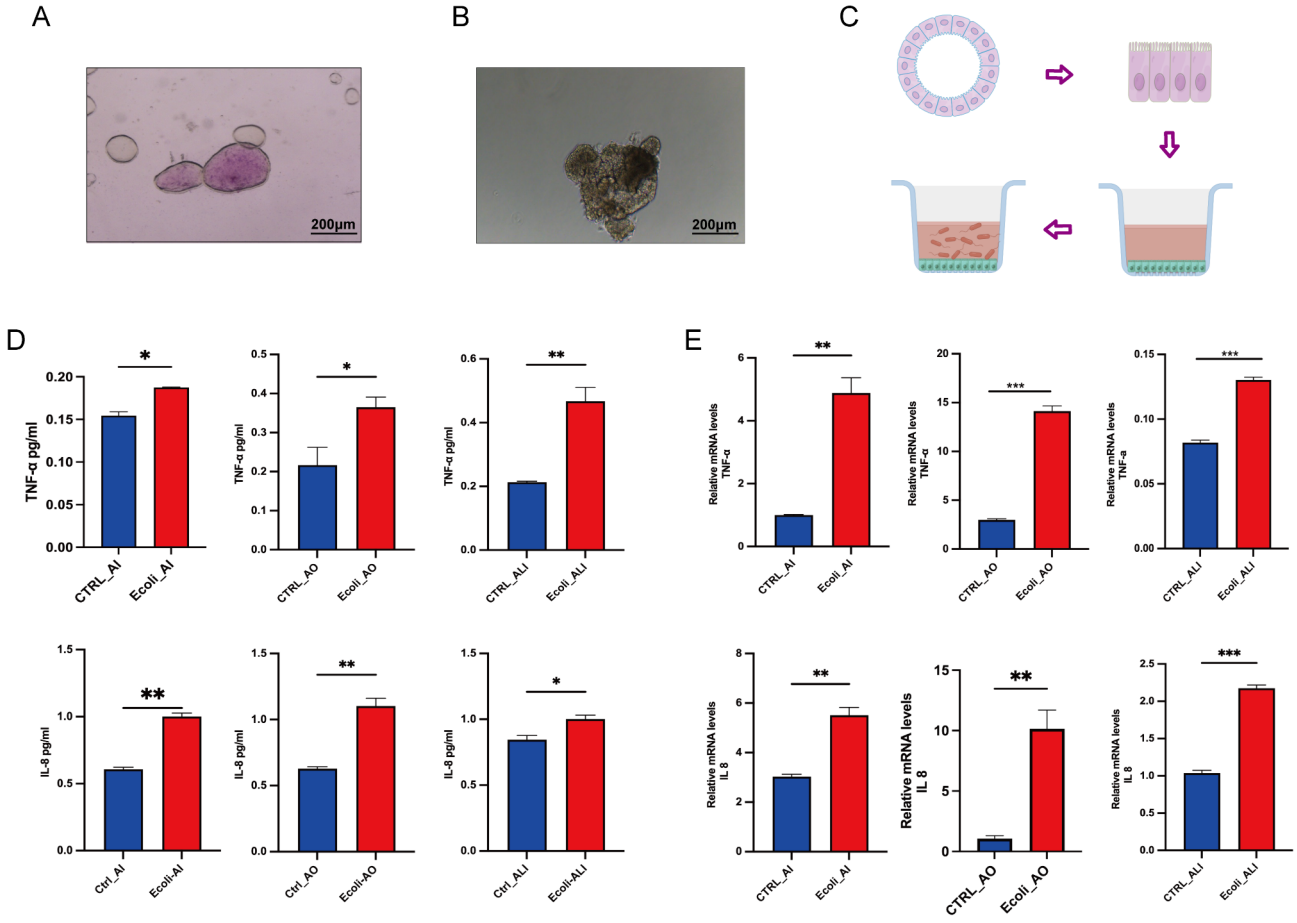

Fig. 3. Comparison of three infection models. (**A**) *Organoid microinjection*: After staining *E. coli*, the bacteria were injected into the organoids using a microinjection technique. Scale bar: 200 μm. (**B**) *Apical-out infection*: After removing the Matrigel, organoids with an apical-out orientation were infected with *E. coli*. *E. coli* can be observed adhering to the surface of the organoids. (**C**) *Organoid ALI culture model*: After removing the Matrigel, the organoids were dissociated into cell clusters and seeded into Transwell chambers. After several days of culture, the organoids were infected with *E. coli*. (**D**) ELISA assay measuring the expression of inflammatory factors. (**E**) RT-qPCR analysis of mRNA expression levels of inflammatory factors. The results shown are representative of three independent experiments. Data are presented as means ± SEM. Statistical significance is indicated as follows: $^{*}P \leq 0.05$, $^{**}P \leq 0.01$, $^{***}P \leq 0.001$.

Discussion

This study provides valuable insights into pathogen-host interactions within endometrial tissue, with significant clinical implications. The three models—organoid, ALI, and direct infection—each offer unique advantages in replicating infection dynamics, immune responses, and tissue repair. These models present promising platforms for in vitro evaluation of potential therapeutic interventions. To our knowledge, this is the first comparative analysis of different endometrial infection models. Our findings suggest that the direct apical-out infection method closely mirrors the natural infection process, outperforming both microinjection and ALI techniques. This model holds considerable potential for elucidating the mechanisms underlying endometrial infections.

This study highlights the potential for novel therapeutic strategies by examining immune responses and pathogen invasion mechanisms. Targeting specific immune pathways activated during infection could help develop targeted therapies, reducing reliance on broad-spectrum antibiotics and minimizing the risk of resistance. Additionally, the models used in this study could screen drug candidates for their effectiveness in treating endometrial infections, chronic inflammation, and related pathologies. Endometritis, driven by bacterial invasion that disrupts the endometrial epithelial barrier, can lead to a range of detrimental outcomes. With the advancement of assisted reproductive technologies, understanding how pathogenic bacteria influence the endometrial barrier and its receptivity is critical. In vitro models, particularly cell-based systems, have proven essential for investigating host-pathogen interactions and the mechanisms of endometritis. These models provide a controlled platform that mimics human endometrial conditions, enabling studies of immune responses, pathogen evasion, and virulence factors[17–19]. These models enable the study of immune responses, pathogen evasion tactics, and the role of virulence factors in disease progression[20–22]. Moreover, in vitro systems are pivotal for testing the efficacy and toxicity of therapeutic agents during early drug development, potentially decreasing the reliance on costly animal models. Despite increasing interest in advanced culture

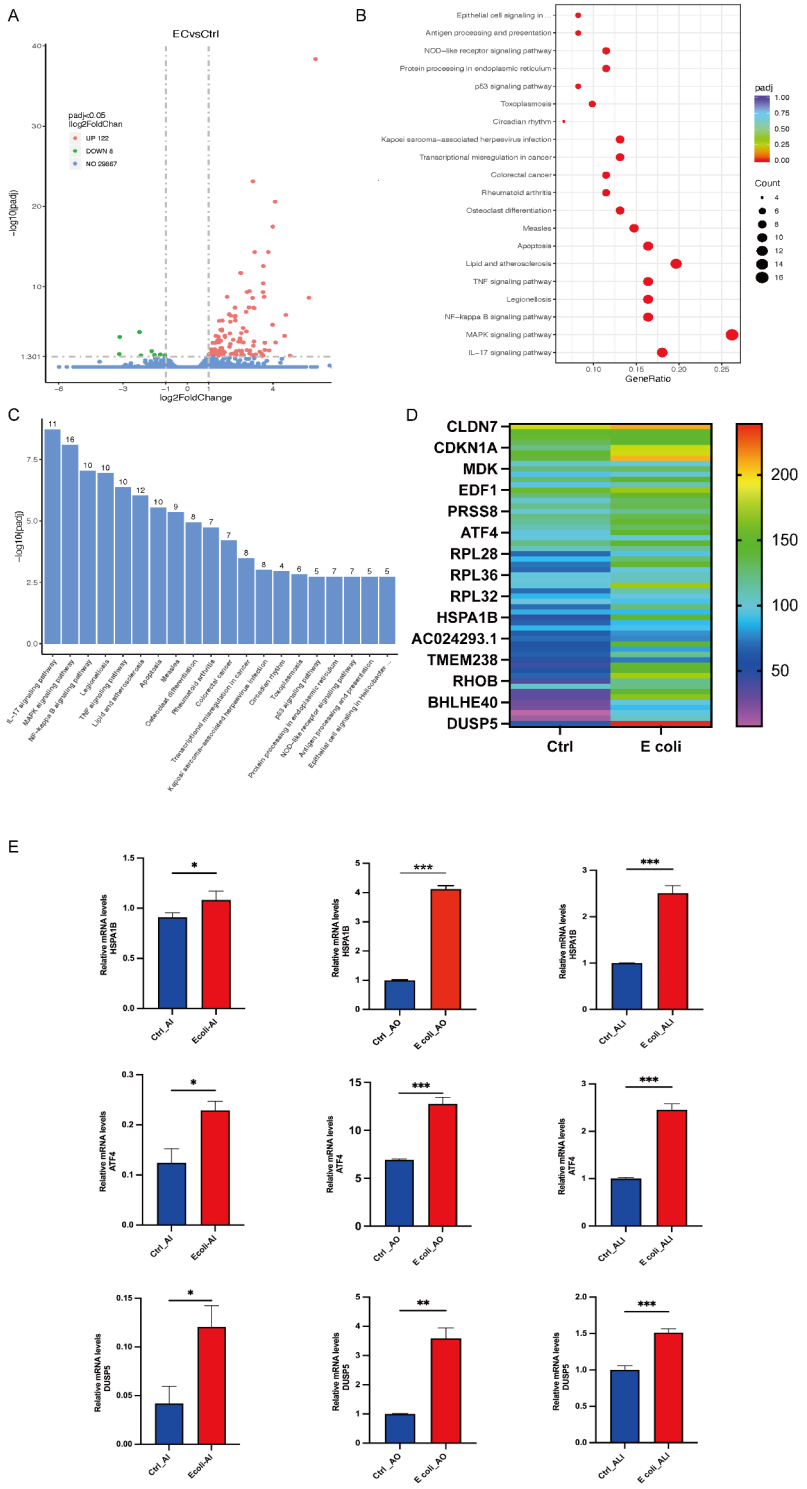

systems for studying endometrial infections, a comprehensive review of these approaches remains limited. Chronic infections, if unresolved, may lead to persistent inflammation in the endometrial tissue, resulting in fibrosis, tissue damage, and impaired repair mechanisms. Such prolonged damage can negatively affect fertility, as the endometrial environment is vital for embryo implantation and pregnancy maintenance. An important area for further investigation is the long-term impact of chronic infections on the endometrial environment and reproductive health, including infertility. While our study focuses on pathogen-host interactions at specific time points, we propose a longitudinal study to assess the progressive nature of tissue damage, immune dysregulation, and cellular dysfunction induced by chronic infections. This approach would provide valuable insights into how prolonged pathogen exposure and immune fluctuations affect endometrial structure and function, contributing to infertility in women with chronic endometritis.

◀**Fig. 4**. Differential gene expression and pathway analysis in organoids infected with *E. coli*. (**A**) Volcano plot displaying differentially expressed genes, with 122 genes upregulated and 8 genes downregulated in *E. coli*-infected organoids compared to the control group. (**B**) Dot plot illustrating key signaling pathway changes in organoids post-infection. Dot size represents the proportion of cells within the cluster expressing a specific gene, while shading indicates relative expression levels (from light to dark). (**C**) KEGG analysis of differentially expressed mRNA target genes, presenting a bar chart of the top 20 KEGG pathways with upregulated genes. KEGG: Kyoto Encyclopedia of Genes and Genomes. (**D**) Hierarchical clustering of significantly regulated genes (2-fold change, FDR $P < 0.05$) comparing *E. coli*-infected organoids to controls. (**E**) RT-PCR analysis of RNA isolated from organoid cultures, as described in the methods section. Relative mRNA levels of *HAPA1B*, *ATF4*, and *DUSP5* in *E. coli*-treated organoids are shown. Results represent the mean ± SEM of triplicate samples, representative of three independent experiments. Statistical significance is denoted as follows: $^{*}P \leq 0.05$, $^{**}P \leq 0.01$, $^{***}P \leq 0.001$.

Organoid models effectively simulate the three-dimensional structure and cellular diversity of original tissues. Derived from progenitor or stem cells, these models self-organize, making them highly suitable for studies on disease mechanisms, tissue development, and host-pathogen interactions. Due to their close resemblance to in vivo conditions, particularly with respect to epithelial barriers, organoids have become instrumental in infection research[23,24]. However, reversed polarity in endometrial organoids poses certain limitations for studying infections. For instance, while Escherichia coli can be introduced directly into Matrigel-embedded organoids using microinjection, the bacteria often remain confined within the lumen. This leads to significant structural damage within the organoid, effectively demonstrating bacterial virulence as observed in vivo. Nevertheless, damage to the epithelial surface typically manifests at a later stage, and this localized infection does not fully capture the physiological progression of pathogens in endometrial infections. Furthermore, the microinjection process itself is technically demanding, requiring specialized personnel and equipment. Given that each droplet of Matrigel can only house a small number of organoids, scalability remains limited. The time-consuming nature of the injection procedure, coupled with the restricted number of organoids that can be processed, presents further challenges for broader application.

The ALI model creates a simplified and controlled environment, exposing epithelial cells to air on one side and culture medium on the other, closely replicating in vivo epithelial surface conditions. This system is particularly beneficial for studying barrier tissues, such as the airways. By growing cells in a two-dimensional monolayer, it allows for direct pathogen interaction on the apical surface, providing an efficient platform for infection research and enabling detailed observation of cellular responses, including the secretion of cytokines and chemokines. ALI models, for example, often exhibit a heightened immune response post-infection, with increased production of pro-inflammatory cytokines like TNF-α and IL-8, especially when comparing infection techniques like direct injection versus ALI infection. However, a limitation of ALI models is their lack of the three-dimensional architecture seen in organoids, which may limit their ability to fully replicate the complex cellular interactions found in a tissue-like environment.

ALI culture system has significantly advanced the understanding of host-pathogen interactions, particularly in airway models. Its ability to provide access to both the apical and basal surfaces while maintaining a cellular composition that closely mimics in vivo tissues has greatly facilitated the investigation of pathogen-associated diseases in the respiratory tract airway[25,26]. However, adapting this system for endometrial studies poses unique challenges. One limitation is its scalability, which is hindered by its dependence on permeable membrane tissue culture inserts, making high-throughput applications difficult. Additionally, the prolonged culture time, often requiring 3 to 4 weeks for cellular differentiation, coupled with the inability to continuously monitor cellular changes post-infection, limits its effectiveness in endometrial research. Furthermore, the limited passage capability of primary endometrial cells before losing key functional characteristics, such as differentiation potential, adds complexity and increases costs for sourcing cells. Media variations, recently noted in airway models, may also affect ALI performance, requiring time-consuming pre-validation steps. The rigid porous membranes of ALI transwell inserts, typically made from polyethylene terephthalate (PET), may introduce physical stress to cells, which can interfere with epithelial differentiation due to the mechanical mismatch at the interface.

Translating insights from experimental models into clinical trials is crucial for validating therapeutic interventions. To accelerate the discovery and testing of novel therapeutics, optimizing infection models like organoid and ALI models to better replicate chronic infection scenarios is essential. Future studies should focus on identifying pathogen-specific virulence factors, such as adhesins, toxins, and other key molecules that drive infection and immune evasion. Targeting these factors could provide a more targeted and effective approach to treating gynecological infections, minimizing collateral tissue damage. Given the central role of immune responses in chronic endometrial infections, research should prioritize immunomodulatory therapies to control excessive inflammation and tissue damage. Targeting inflammatory cytokines, such as IL-6 and TNF-α, could offer new strategies for mitigating chronic infection effects on the endometrium and improving fertility outcomes in affected individuals. Although this study focuses on endometrial organoids, the insights gained are applicable to organoids derived from other epithelial tissues, such as the mammary gland, esophagus, small intestine, and colon. These organoids, exhibiting polarity reversal, could benefit from the infection modeling techniques discussed here. Our research contributes to advancing infection models in organoid studies and highlights the potential of organoid-based models for translational applications across various epithelial tissues. Moreover, endometrial organoid models can improve preclinical drug development by identifying therapeutic

compounds before clinical trials. Insights into pathogen-host interactions could also guide personalized treatment approaches, particularly for patients with recurrent or chronic endometrial infections.

Conclusions

A suitable model is crucial for the study of endometrial infections. We compared three models: microinjection, direct infection, and the air-liquid interface (ALI) model. Although microinjection allows for precise delivery, it is technically challenging and requires specialized equipment, making the procedure complex. The ALI model, while effective, involves a prolonged culture period, and direct observation of cell growth is not feasible throughout the process. In contrast, the direct infection method, which simply involves the removal of Matrigel, is straightforward, cost-effective, and allows for real-time monitoring of cell dynamics. However, despite its advantages, the direct infection approach has limitations that require further refinement.

Data availability

The datasets generated and/or analyzed during the current study are available in the GEO repository, GSE283460.

Received: 1 November 2024; Accepted: 6 March 2025
Published online: 12 March 2025

References

1. Kitaya, K., Takeuchi, T., Mizuta, S., Matsubayashi, H. & Ishikawa, T. Endometritis: New time, new concepts. *Fertil. Steril.* **110**, 344–350. https://doi.org/10.1016/j.fertnstert.2018.04.012 (2018).
2. Kitaya, K., Tanaka, S. E., Sakuraba, Y. & Ishikawa, T. Multi-drug-resistant chronic endometritis in infertile women with repeated implantation failure: Trend over the decade and pilot study for third-line oral antibiotic treatment. *J. Assist. Reprod. Genet.* **39**, 1839–1848. https://doi.org/10.1007/s10815-022-02528-7 (2022).
3. Shen, Y., Wang, Y., Wang, S., Li, C. & Han, F. J. Research progress on the application of organoids in gynecological tumors. *Front. Pharmacol.* **15**, 1417576. https://doi.org/10.3389/fphar.2024.1417576 (2024).
4. Guo, J. et al. Using organoids to investigate human endometrial receptivity. *Front. Endocrinol. (Lausanne).* **14**, 1158515. https://doi.org/10.3389/fendo.2023.1158515 (2023).
5. Ahmad, V., Yeddula, S. G. R., Telugu, B. P., Spencer, T. E. & Kelleher, A. M. Development of polarity-reversed endometrial epithelial organoids. *Reproduction* **167**, e230478. https://doi.org/10.1530/REP-23-0478 (2024).
6. Hariss, F. et al. Cytotoxic innate intraepithelial lymphocytes control early stages of Cryptosporidium infection. *Front. Immunol.* **14**, 1229406. https://doi.org/10.3389/fimmu.2023.1229406 (2023).
7. Pinto, S. et al. Nanoparticles targeting the intestinal Fc receptor enhance intestinal cellular trafficking of semaglutide. *J. Controlled Release.* **366**, 621–636. https://doi.org/10.1016/j.jconrel.2024.01.015 (2024).
8. Mahieu, L., Van Moll, L., De Vooght, L. & Delputte, P. Cos. In vitro modelling of bacterial pneumonia: A comparative analysis of widely applied complex cell culture models. *FEMS Microbiol. Rev.* **48**, fuae007. https://doi.org/10.1093/femsre/fuae007 (2024).
9. Fitzgerald, H. C., Dhakal, P., Behura, S. K., Schust, D. J. & Spencer, T. E. Self-renewing endometrial epithelial organoids of the human uterus. *Proc. Natl. Acad. Sci. U. S. A.* **116**, 23132–23142. https://doi.org/10.1073/pnas.1915389116 (2019).
10. Portugal, J. et al. Toxicity of airborne nanoparticles: Facts and challenges. *Environ. Int.* **190**, 108889. https://doi.org/10.1016/j.envint.2024.108889 (2024).
11. Ramirez-Moral, I. et al. Single-cell transcriptomics reveals subset-specific metabolic profiles underpinning the bronchial epithelial response to Flagellin. *iScience* **27**, 110662. https://doi.org/10.1016/j.isci.2024.110662 (2024).
12. Chen, L. et al. Inflammation-induced loss of CFTR-expressing airway ionocytes in non-eosinophilic asthma, respirology N/a (n.d.). https://doi.org/10.1111/resp.14833
13. F, G. M. M. G. C. et al. On the dose-response association of fine and ultrafine particles in an urban atmosphere: Toxicological outcomes on bronchial cells at realistic doses of exposure at the air liquid interface. *Chemosphere* **366** https://doi.org/10.1016/j.chemosphere.2024.143417 (2024).
14. Wang, Y. et al. SARS-CoV-2-infected human airway epithelial cell cultures uniquely lack interferon and immediate early gene responses caused by other coronaviruses. *Clin. Transl. Immunol.* **13**, e1503. https://doi.org/10.1002/cti2.1503 (2024).
15. Lacroix, G., Gouyer, V., Rocher, M., Gottrand, F. & Desseyn, J. L. A porous cervical mucus plug leads to preterm birth induced by experimental vaginal infection in mice. *iScience* **25**, 104526. https://doi.org/10.1016/j.isci.2022.104526 (2022).
16. Brunham, R. C., Gottlieb, S. L. & Paavonen, J. Pelvic inflammatory disease. *N. Engl. J. Med.* **372**, 2039–2048. https://doi.org/10.1056/NEJMra1411426 (2015).
17. Turco, M. Y. et al. Long-term, hormone-responsive organoid cultures of human endometrium in a chemically defined medium. *Nat. Cell. Biol.* **19**, 568–577. https://doi.org/10.1038/ncb3516 (2017).
18. Tang, S., Parks, S. E., Liao, Z., Cope, D. I. & Blutt, S. E. D. Monsivais. Establishing 3D endometrial organoids from the mouse uterus (2023). https://doi.org/10.3791/64448
19. Luddi, A. et al. Organoids of human endometrium: A powerful in vitro model for the Endometrium-Embryo Cross-Talk at the implantation site. *Cells* **9**, 1121. https://doi.org/10.3390/cells9051121 (2020).
20. Rodriguez-Valverde, D. et al. Highly-conserved regulatory activity of the ANR family in the virulence of diarrheagenic bacteria through interaction with master and global regulators. *Sci. Rep.* **13**, 7024. https://doi.org/10.1038/s41598-023-33997-0 (2023).
21. Zhou, L. F., Liao, H. Y., Han, Y. & Zhao, Y. The use of organoids in creating immune microenvironments and treating gynecological tumors. *J. Transl Med.* **22**, 856. https://doi.org/10.1186/s12967-024-05649-y (2024).
22. Tang, M. et al. Evaluating bacterial pathogenesis using a model of human airway organoids infected with pseudomonas aeruginosa biofilms. Microbiol Spectr 10 (n.d.) e02408-22. https://doi.org/10.1128/spectrum.02408-22
23. Karthaus, W. R. et al. Identification of multipotent luminal progenitor cells in human prostate organoid cultures. *Cell* **159**, 163–175. https://doi.org/10.1016/j.cell.2014.08.017 (2014).
24. Clevers, H. Modeling development and disease with organoids. *Cell* **165**, 1586–1597. https://doi.org/10.1016/j.cell.2016.05.082 (2016).
25. van der Horst, D. et al. Large-scale deep learning identifies the antiviral potential of PKI-179 and MTI-31 against coronaviruses. *Antiviral Res.* **231**, 106012. https://doi.org/10.1016/j.antiviral.2024.106012 (2024).
26. He, N., Ms, R., Y, J., D, K. & Jh, S. Differential regulation of viral entry-associated genes modulated by inflammatory cytokines in the nasal epithelium. *J. Med. Virol.* **96** https://doi.org/10.1002/jmv.29913 (2024).

Acknowledgements

The figures were created By Figdraw.

Author contributions
XZ conducted the research and drafted the manuscript. LZ assisted in the revision of the manuscript and the construction of figures and tables. ZHL and LYF contributed to the conceptual framework, supervised the study, and revised the manuscript. All authors read and approved the final manuscript.

Funding
R&D Program of Beijing Municipal Education Commission (KM202410025006).

Declarations

Competing interests
The authors declare no competing interests.

Ethics approval and consent to participate
This study was conducted in accordance with the Declaration of Helsinki. All analyses involving patient and human samples followed the norms and procedures of the Beijing Obstetrics and Gynecology Hospital, Capital Medical University.

Consent for publication
All authors consent to publication.

Additional information
Correspondence and requests for materials should be addressed to L.F. or Z.L.